

Deciphering the Olefin Isomerization-Polymerization Paradox of Palladium(II) Diimine Catalysts: Discovery of Simultaneous and Independent Pathways of Olefin Isomerization and Living Polymerization

Dung Nguyen, Shengguang Wang, Lars C. Grabow,* and Eva Harth*



Cite This: <https://doi.org/10.1021/jacs.3c01513>



Read Online

ACCESS |



Metrics & More

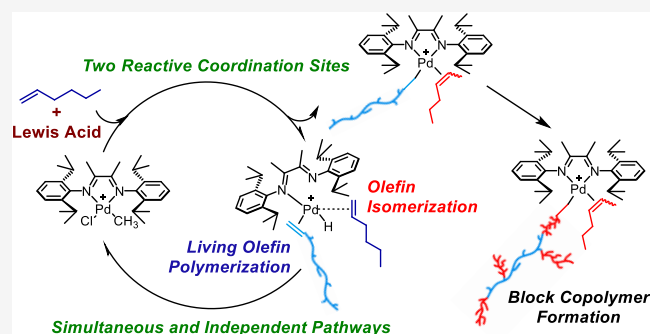


Article Recommendations



Supporting Information

ABSTRACT: This work elucidates a long-standing unexplained paradox commonly observed within the polymerization of α -olefin using palladium (Pd)(II)–diimine catalysts, in which isomerization and living polymerization of α -olefins are both observed. With a classical mechanistic understanding of these complexes, this behavior is often dismissed and interpreted as experimental error. Herein, we present a comprehensive mechanistic investigation into this phenomenon that supports the existence of a novel mechanistic pathway for Pd(II)–diimine complexes. Part one of the mechanistic study lays the foundation of the proposed mechanism, in which neutral Pd(II)–diimine complexes were found to exhibit a moderate to good catalytic activity for olefin isomerization of α -olefins despite the established notion that catalyst activation is required. Extensive experimental and computational studies reveal the possibility of a partial dissociation of the diimine ligand, which frees up one coordination site and enables coordination–insertion. This finding is significant as the coexistence of two reactive coordination sites at the palladium center becomes a valid proposal for the activated cationic Pd(II)–diimine complexes. In part two, we examined and validated the simultaneously observed α -olefin isomerization and living polymerization using the cationic Pd(II)–diimine catalyst, which supports the presence of two independent reaction pathways of isomerization and polymerization, respectively. Moreover, the addition of a strong Lewis acid, such as AlCl_3 , accelerates the ligand dissociation and the consequential isomerization as it weakens the palladium–nitrogen bond through competitive binding. In part three, Lewis acid-triggered olefin isomerization-polymerization is employed to prepare living olefinic block copolymers and further synthesize novel polyolefin-polar block copolymers with unique architectures, distinct levels of branching, crystallinity, and polar functionality in a one-pot manner.



INTRODUCTION

Late transition metal catalysis for olefin polymerization has remained one of the most intensively studied areas of research, especially since Brookhart and co-workers successfully developed α -diimine nickel and palladium complexes capable of living olefin polymerization as well as copolymerization with polar monomers due to their relatively low oxophilicity.^{1–5} Since then, α -diimine nickel and palladium complexes have been studied extensively, and detailed mechanistic investigation has provided valuable insights and a core understanding of the catalyst designs as well as the mechanism of the chain propagation, chain-walking, and chain transfer processes.^{1,5–15} Particularly, the original complexes' key design feature is the axial steric bulk from the ortho-aryl substituents, which retards chain transfer significantly to afford high molecular weight polymers instead of isomers, dimers, or oligomers.^{16–24} While this effectively eliminates undesired side reactions to ethylene polymerization, isomerization of α -olefin

to internal olefins is surprisingly still a commonly observed side reaction to α -olefin polymerization, particularly by employing traditional Brookhart-type palladium catalysts.²⁵ For instance, Brookhart and co-workers reported that living polymerization of 1-hexene at 0 °C using the Pd(II)–diimine catalyst observed 29% of the remaining 1-hexene isomerized to 2-hexene and 3-hexene after 3 h (Figure 1).²⁶ Interestingly, the kinetics showed that 1-hexene was consumed toward polymerization and isomerization simultaneously without affecting the livingness of the polymerization. The isomerization was acknowledged as a “complication”, and no mechanism was

Received: February 9, 2023



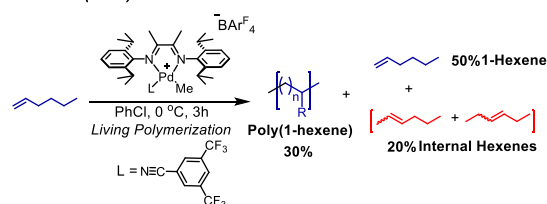
ACS Publications

© XXXX American Chemical Society

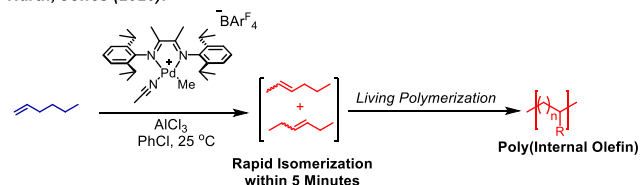
A

<https://doi.org/10.1021/jacs.3c01513>
J. Am. Chem. Soc. XXXX, XXX, XXX–XXX

Brookhart (2003):



Harth, Jones (2020):



Harth (2021):

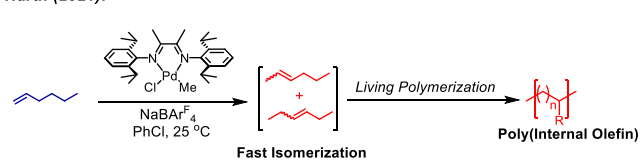


Figure 1. Observed phenomenon of olefin isomerization-polymerization from previous works.

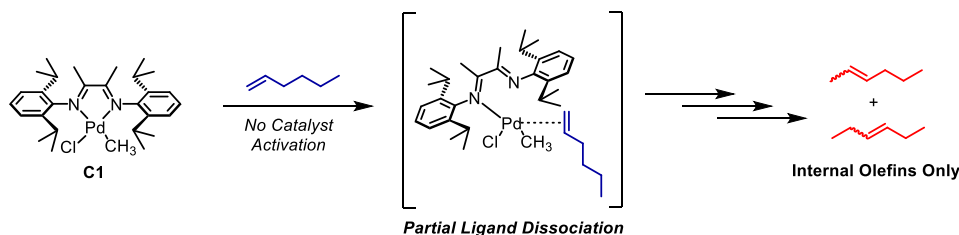
provided.^{25,27} Since then, this phenomenon of simultaneous α -olefin isomerization-polymerization has been observed within different palladium catalyst systems, but the isomerization has simply been acknowledged as a competing reaction due to the

non-livingness of those systems and thus remained unexplained.^{28–30}

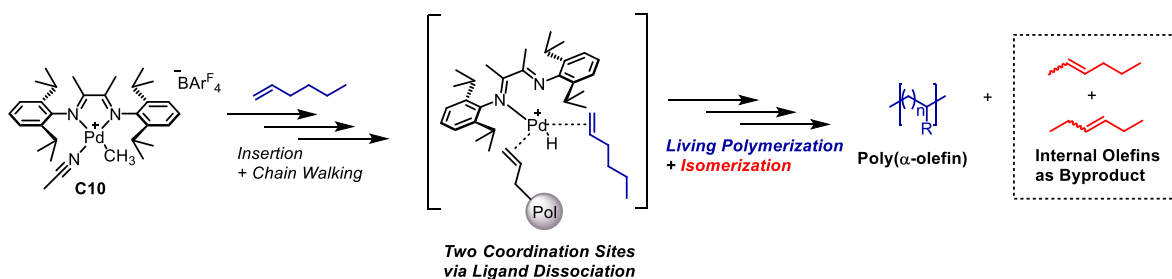
In 2020, Harth, Jones, and co-workers reported a new method of Lewis acid-triggered olefin isomerization-polymerization, in which this phenomenon of observable isomerization within living polymerization of α -olefin becomes significantly more pronounced in the presence of a Lewis acid (Figure 1).³¹ Herein, the combination of AlCl_3 and the traditional Brookhart cationic $\text{Pd}(\text{II})$ -diimine complex could trigger rapid in situ isomerization of α -olefin on demand, and complete isomerization can be achieved in as fast as 5 min followed by the accelerated living polymerization of internal olefins. Similarly, we demonstrated that in situ activation of the precatalyst with sodium tetrakis[3,5-bis(trifluoromethyl)phenyl]borate (NaBAR_4^F) also exhibits the same isomerization-polymerization behavior, albeit with a slightly slower rate of polymerization possibly due to the absence of a Lewis acid (Figure 1).³² Nevertheless, living polymerization was still observed in both cases, indicating that the isomerization process is not a conventional competing reaction, which typically results in chain transfer and non-living polymerization. Moreover, it also raises the question of how it is feasible for olefin isomerization and, even more so, rapid isomerization in the presence of a Lewis acid to occur, given the catalyst design, which has proven to be very effective at limiting chain transfer.

As a result, we assumed that there is an unexplored mechanistic pathway involved in the olefin isomerization process, which is both greatly enhanced in the presence of a Lewis acid and independent of the well-established olefin

Part 1: Palladium-Catalyzed Olefin Isomerization Using Neutral Complexes



Part 2: Simultaneous Living Olefin Polymerization and Olefin Isomerization Initiated at Two Different Coordination Sites



Part 3: Block Copolymer Synthesis via a Tandem of Lewis Acid-Triggered Olefin Isomerization-Polymerization and MILRad Polymerization

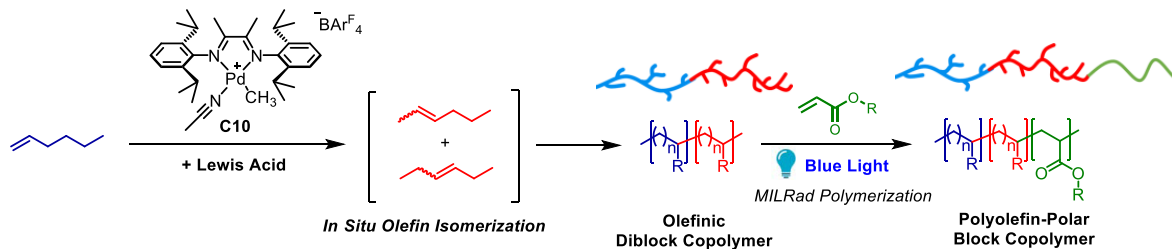


Figure 2. Outline for this work's mechanistic study divided into three segments.

insertion-polymerization pathway. Specifically, we hypothesize that there are actually two active coordination sites on the metal center instead of the classical belief of a single active coordination site. Herein, each coordination site would be responsible for isomerization and polymerization individually, which ensures no chain transfer and thus living polymerization. The second active site would be generated *via* partial dissociation of the diimine ligand, which is accelerated in the presence of a stronger Lewis acid than Pd(II). This work provides a detailed rationale for this proposal and an extensive investigation into this mechanism, which fully explains the inherent olefin isomerization-polymerization behavior of the Pd(II)–diimine catalyst for the first time. Specifically, isomerization of various α -olefins was observed using different “nonactivated” neutral Pd(II)–diimine complexes, and the density functional theory (DFT) study supports the possibility of ligand dissociation and thus freeing up one coordination site. The observation of simultaneous isomerization and living polymerization of α -olefins using cationic Pd(II) diimine complexes, especially in the presence of a Lewis acid, suggests the presence of two coordination sites, which agrees with the hypothesis of ligand dissociation. Consequently, the living and simultaneous isomerization-polymerization give ground to the formation of complex olefinic block copolymer (OBC) architectures. Moreover, di- and triblock polyolefin-acrylate copolymers were synthesized *via* metal-organic insertion/light-initiated radical (MILRad) polymerization.³³ We envision a highly tunable catalyst system, in which the Brookhart Pd(II)–diimine catalyst’s activity can be easily tuned *via* external stimuli such as Lewis acids and light irradiation, that is capable of synthesizing unique block copolymers with various levels of branching, crystallinity, and polar functionality.

■ RESULTS AND DISCUSSION

The scope of this paper will be divided into three sections (Figure 2). Part 1 will explore the nonactivated neutral Brookhart-type Pd(II)–diimine catalyst’s unexpected reactivity for olefin isomerization and its proposed mechanism involving a partial dissociation of the diimine bidentate ligand. Part 2 will focus on the mechanism of olefin isomerization-polymerization by investigating the two simultaneous catalytic cycles of olefin isomerization and living olefin polymerization, which involves two independent reactive coordination sites within a single catalytic species. Finally, part 3 will investigate the photo-initiated “switch” from olefin isomerization-polymerization to MILRad polymerization for the synthesis of polyolefin-polar block copolymers.

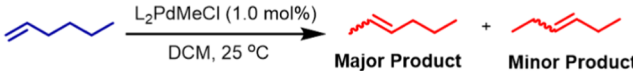
Specifically, in part 1, olefin polymerization using a neutral Pd(II)-diimine precatalyst was studied by investigating the influences of cocatalysts’ Lewis acidity on the catalyst activity. The proposed mechanism is then deduced experimentally from three possible hypotheses *via* ligand screening. Additionally, density functional theory (DFT) calculations are also employed to further corroborate this mechanism. In part 2, the livingness of the polymerization as well as the two simultaneous processes of isomerization and polymerization are thoroughly studied through nuclear magnetic resonance (NMR), gel permeation chromatography (GPC), and kinetic analyses. Moreover, the mechanism of the olefin isomerization-polymerization phenomenon is proposed and expanded in agreement with the kinetic data as well as the mechanism from part 1. In part 3, different Lewis acids are screened and optimized for the switch to MILRad polymerization. Different

α -olefins such as 1-hexene, 1-decene, and 1-octadecene, along with different acrylates, are also used to synthesize a series of block copolymers with varying levels of branching, crystallinity, and unique architectures.

Part 1: Palladium-Catalyzed Olefin Isomerization Using a Neutral Pd(II)–Diimine Catalyst. As discussed earlier, rapid α -olefin isomerization was reported by our group with both the combinations of the cationic complex and AlCl_3 , as well as the in situ activation of the precatalyst and $\text{NaBAR}_4^{\text{F}}$ (Figure 1). In the same studies, it was also determined that the two reactions most likely involve the same mechanism, in which the exclusion of the ancillary ligand acetonitrile (MeCN) *via* either abstraction by a Lewis acid or simple omission from the reaction is the key to trigger isomerization.^{31,32} However, the difference in the rate of isomerization between the two reactions possibly implies that the Lewis acidity and isomerization rate have a positive correlation. Hence, we decided to use cocatalysts with different Lewis acidities to activate precatalyst C1 in situ in the absence of MeCN for the polymerization of 1-hexene in order to analyze the rate of olefin isomerization (Table S1). Predictably, complete isomerization of 1-hexene to 2-hexene and 3-hexene was observed within 5 min in the presence of AlCl_3 , a strong Lewis acid, while it took 15 min to achieve similar results for $\text{NaBAR}_4^{\text{F}}$, $\text{AgBAR}_4^{\text{F}}$, AgPF_6 , or AgBF_4 , which further correlates that the Lewis acidity of a cocatalyst strongly influences the rate of olefin isomerization. Additionally, NaAlCl_4 , NaPF_6 , and NaBF_4 were also employed as cocatalysts to compare against their Al and Ag analogues due to their much weaker Lewis acidity to further test the effects of Lewis acid on olefin isomerization. Confoundingly, while complete olefin isomerization was achieved in all three cases, no subsequent polymerization of the generated internal hexenes was observed. In other words, this observed result opens a significant Pandora’s box because it demonstrates that the catalyst’s activity can be completely tuned from olefin isomerization-polymerization to olefin isomerization simply by using different cocatalysts without any ligand modifications. However, this observation is not consistent with our current mechanistic understanding because in situ activations of C1 using these analogue pairs of cocatalysts should form identical cationic active species, and thus, they should yield similar catalytic activities. Therefore, it was conjectured that C1 is possibly not activated by the NaX ($\text{X} = [\text{AlCl}_4]^-$, $[\text{PF}_6]^-$, and $[\text{BF}_4]^-$) cocatalyst and that the nonactivated neutral complex C1 remains the active species that isomerize α -olefin to internal olefins readily without further polymerization. This behavior is not expected from these types of complexes because they are usually considered to be fairly stable due to their square planar geometry and saturated 16-electron configuration without any highly labile metal–ligand bond for further olefin coordination–insertion. However, a control reaction of C1 with 1-hexene indeed resulted in complete isomerization of 1-hexene to 2-hexene (80%) and 3-hexene (20%) within 2 h. On the other hand, further control experiments of 1-hexene isomerization using C1 in the presence of H_2O resulted in minimal isomerization of 1-hexene, indicating that the precatalyst was not activated by H_2O , which has been previously demonstrated to be a possible activation pathway for Pd(II)–diimine catalysts (Figure S4).^{34–37} As a result, these findings confirm the unlikely hypothesis that the nonactivated Pd(II)–diimine neutral complex inherently exhibits some catalytic cycle toward olefin isomerization.

Upon this discovery, various neutral Pd(II) complexes were synthesized using different types of ligands, including diphosphine, diamine, and diimine, to further investigate the scope as well as the effects of ligands on the catalyst activity and the reaction mechanism (Supporting Information, SI Section S2). The results of 1-hexene isomerization using these complexes are summarized in Table 1, as the reactions were

Table 1. Ligand Screening for Palladium-Catalyzed Olefin Isomerization Using Neutral Complexes



Entry ^[a]	Catalyst	Ligand	Yield (%) ^[b]	TOF (h ⁻¹)
1	C1		72 ^[c]	72
2	C2		21 ^[d]	7
3	C3		47 ^[c]	47
4	C4		64 ^[e]	4
5	C5		7 ^[e]	0.44
6	C6		No reaction ^[e]	
7	C7		5 ^[e]	0.31
8	C8		No reaction ^[e]	
9	C9		No reaction ^[e]	

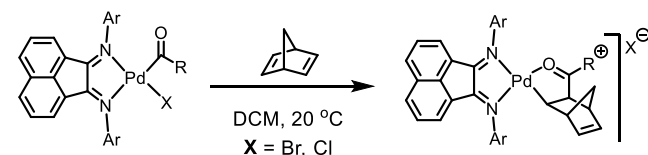
^aReaction conditions: 0.02 mmol of catalyst, 0.2 mmol of 1-hexene, 3 mL of chlorobenzene at 25 °C. ^bThe yields were calculated using ¹H NMR. ^cThe reactions were quenched using Et₃SiH after 1 h. ^dThe reactions were quenched using Et₃SiH after 3 h. ^eThe reactions were quenched using Et₃SiH after 16 h.

carried out with a catalyst loading of 1 mol % at room temperature (25 °C) in dichloromethane (DCM). Interestingly, catalyst C4, which was purchased and used as is for the synthesis of other catalysts, exhibits moderate catalytic activity for 1-hexene isomerization with a turnover frequency (TOF) of 4 h⁻¹. On the other hand, no reaction was observed for P,P-complexes C8 and C9 as well as N,N-complex C6, while other N,N-complexes C5 and C7 show significantly poorer activities than that of C4 with a TOF of only 0.44 and 0.31 h⁻¹, respectively. Of all the studied catalysts, diimine complexes demonstrate the best catalytic activity for olefin isomerization, especially for catalysts C3 and C1 with a TOF of 47 and 72 h⁻¹, respectively, while catalyst C2's activity (TOF = 7 h⁻¹) is only comparable to that of C4. It is indeed unexpected that C1, whose axial steric bulk hinders chain transfer the most significantly, works better than both C2 and C3 with little to no axial steric bulk.

Mechanistic Rationale. It is a rather intriguing yet crucial finding that neutral Pd(II)–diimine complexes readily isomer-

ize α -olefins to internal olefins without any activation to generate an open coordination site because it indicates that these complexes' catalytic activity most likely involves a new mechanistic pathway. Notably, Vrieze et al. have reported precedents of neutral acylpalladium complexes bearing similarly rigid diimine ligands that react with norbornadiene *via* migratory insertion to form isolable cationic alkylpalladium complexes with the dissociated halide counteranion (Figure 3).³⁸ The suggested key mechanistic steps for the reaction

Vrieze (1996): Reaction of neutral acylpalladium(II) complexes with norbornadiene



Albano, Vitagliano (1990): Synthesis of five-coordinate olefin-palladium(II) complexes

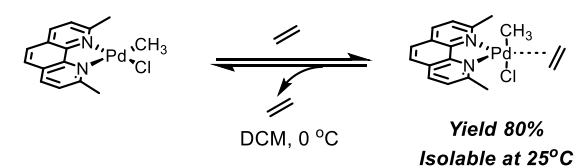


Figure 3. Reactions of neutral palladium complexes with olefins demonstrated by previous works.

involve solvent-assisted dissociation of either nitrogen or halide followed by olefin association and insertion. Additionally, the second proposed pathway would involve the migratory insertion of olefin in a contact ion pair intermediate, which might be formed *via* olefin association followed by either nitrogen or halide dissociation. However, there is no mention of a possible catalytic behavior or olefin insertion directly into the Pd–alkyl bond instead of the Pd–acyl bond, possibly due to the lack of the chelate effect from the carbonyl group to stabilize the complex.

As the reaction involves only the neutral Pd(II)–diimine catalyst and α -olefin, there are three possible mechanistic hypotheses that can explain how a coordination site is generated to initiate the isomerization of α -olefin (Figure 4). The first plausible mechanism hypothesizes the disassociation of chloride from the Pd center to form a cationic Pd complex with a chloride counteranion, which is then followed by olefin coordination and insertion. However, this hypothesis is contradicted by our ligand screening results. Based on this hypothesis, diphosphines and diamines should work better as the ligand for this reaction because they are stronger donors than diimines, thus promoting chloride dissociation more easily. In contrast, Pd-diphosphine complexes C8 and C9 as well as the Pd–diamine complex C7 exhibit no catalytic activity, while Pd(II)–diimine complexes readily isomerize α -olefin. Moreover, the subsequent addition of NaBAR₄^F upon the complete isomerization of 1-hexene by complex C1 was observed to initiate olefin polymerization, which shows that the complex was then successfully activated for the classical olefin insertion pathway and that the palladium–chloride bond is not broken during isomerization.

The second hypothesis suggests the formation of a Pd five-coordinate complex as the key intermediate. While funda-

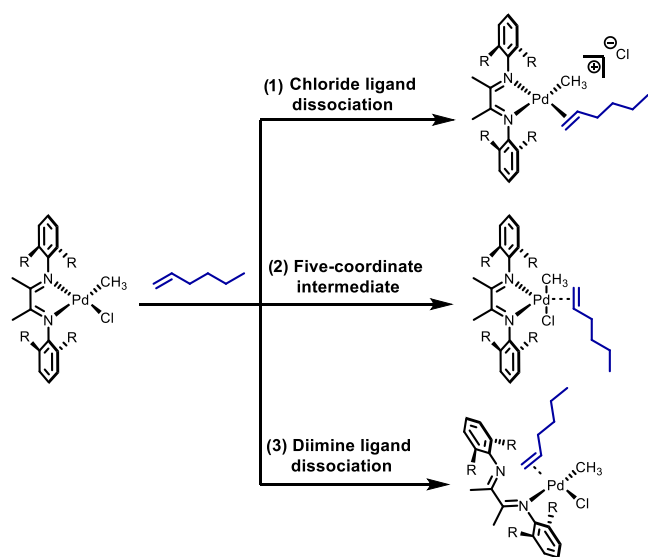


Figure 4. Coordination of 1-hexene to the neutral palladium complex via three different mechanistic pathways.

mental understandings of these complexes indicate that a four-coordinate square planar intermediate is preferable to three-coordinate and five-coordinate intermediates regarding olefin insertion into the metal–hydride bond,³⁹ a five-coordinate intermediate has been previously suggested for the olefin insertion into the Pt–hydride bond.^{40,41} However, the systems used for these examples involve labile monodentate ligands, so it is rather difficult to strongly correlate them to this work. For the second hypothesis, the geometry of the complex should transform from square planar to trigonal bipyramidal instead of square pyramidal because the coordinated olefin and the methyl group have to be on the same plane as well as cis to each other for the subsequent insertion. Obviously, this suggestion remains unlikely because the 16-electron square planar Pd(II)–diimine complex is its most stable and favorable configuration, while there have been no reported isomerization/polymerization mechanisms of Pd(II) catalysts involving a five-coordinate intermediate or a 16-electron-to-18-electron transition. Moreover, attempts to capture the suggested five-coordinate intermediate via ¹H NMR at –80 °C yielded no success, which weakens the argument (Figure S3). On the other hand, it is noteworthy that Vitagliano et al. reported successful syntheses and characterization of multiple five-coordinate trigonal bipyramidal Pd(II) and Pt(II) complexes (Figure 3).^{42–44} However, there were no further reported olefin insertions for these syntheses, and the observed selectivity for the optimized choices of olefins and ligands contradicted the results of this work. Specifically, the more electron-deficient olefins, such as ethylene and maleic anhydride, work better than α -olefin as the coordinated olefin, while complexes with planar steric bulk, such as C6, can form the five-coordinate complex more readily than complex C1 does with axial steric bulk instead.

Finally, the third mechanistic hypothesis proposes partial ligand dissociation of the bidentate diimine ligand, possibly with the assistance of solvent, which would open up one free coordination site for olefin to initiate the isomerization and ensure the more accepted four-coordinate intermediate for the catalytic cycle of olefin isomerization. Although this mechanism is mostly known to hemilabile ligands, an asymmetrical

structure with one stronger and one weaker donor, it has also been proposed by Vrieze et al. for neutral symmetrical Pd(II)–diimine complexes as mentioned earlier. Moreover, the experimental data indeed show a strong correlation to this mechanistic pathway to suggest that it would be the most plausible mechanism for this reaction. As discussed above, complexes with stronger donor ligands, such as diphosphine and diamine, exhibit little to no activity toward olefin isomerization, while ones with weaker donor ligands, like diimine and even cyclooctadiene, demonstrate moderate to great catalytic activity. In other words, one can infer that weaker donor ligands are more easily susceptible to ligand dissociation, so those complexes indeed work better as catalysts for olefin isomerization. Complete displacement of the bidentate ligand with two monodentate α -olefin is unlikely, given that the chelate effect would indicate a much stronger equilibrium shift to ligand recombination instead. However, attempts to capture this intermediate of ligand dissociation remain unsuccessful using spectroscopy like NMR even at as low as –80 °C for this work, which might suggest it to be a transient intermediate (Figures S1 and S2).

Proposed Mechanism. As a result, a complete mechanism is proposed as follows (Figure 5). First, ligand dissociation of **1** opens up a coordination site for the incoming α -olefin, which then swiftly undergoes 2,1-insertion to form the Pd–alkyl intermediate **4**. However, the Pd–alkyl intermediate **4** is highly

Generation of the catalytic Pd–H:

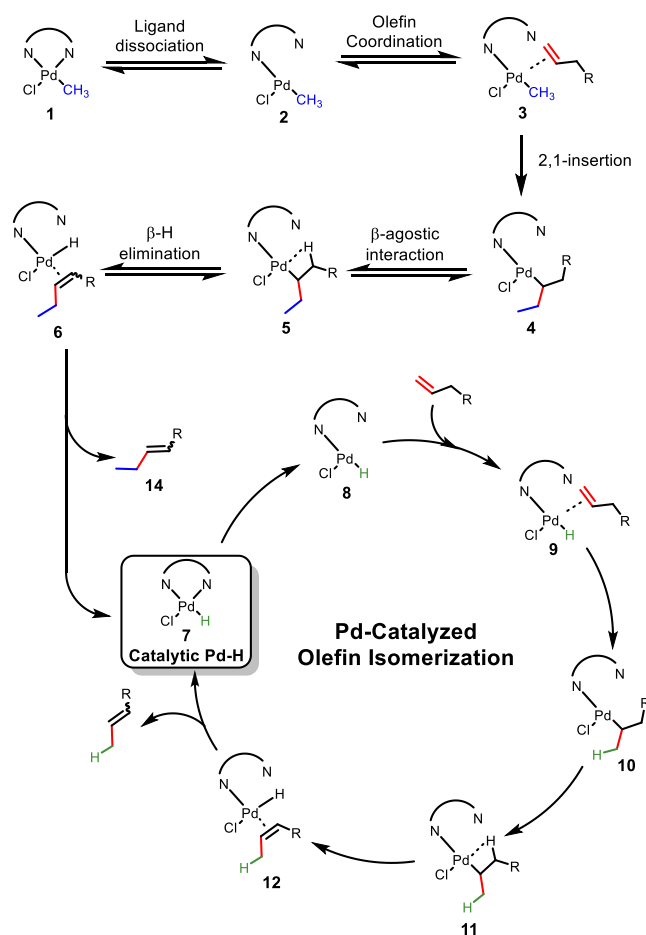


Figure 5. Proposed mechanism for the palladium-catalyzed olefin isomerization using neutral diimine Pd(II) complexes.

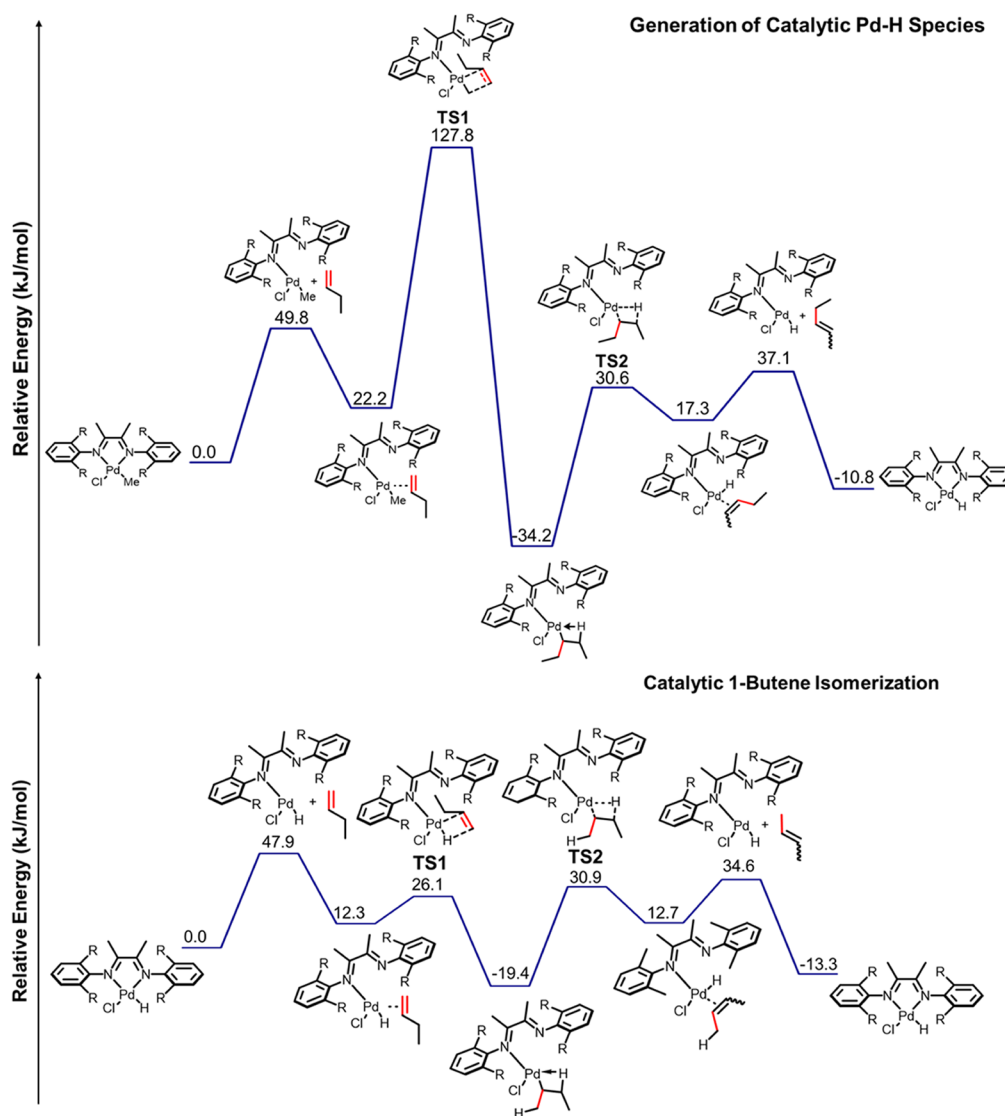


Figure 6. Density functional theory (DFT) calculations of 1-butene isomerization with a neutral diamine Pd(II) complex.

unstable, and the β -agostic interaction of intermediate **5** is favored, which results in further β -hydride elimination reaction and the complexed internal olefin intermediate **6**. Consequently, the N-ligand association is more favorable as the alkylated internal olefin **14** dissociates as a byproduct to yield the catalytic palladium hydride species **7**. The mechanism for the catalytic cycle from **7** remains similar to that of the initiation step: **7** would undergo ligand dissociation for olefin coordination to obtain **9**, which would then undergo successive 2,1-insertion and β -elimination to yield the intermediate of internal olefin π -complex **12**. The internal 2-olefin would then be easily displaced *via* ligand association to regenerate the catalyst **7**, thus completing a cycle of olefin isomerization. However, the catalytic efficiency was observed to be low using ^1H NMR as the characteristic methyl singlet peak of **1** was still observed at 0.5 ppm upon complete isomerization of 1-hexene (Figure S5). Further catalyst activation using $\text{NaBAR}_4^{\text{F}}$ resulted in polymers with a bimodal molecular weight distribution (MWD), which suggests the presence of both catalytic Pd-hydride species **7** and unreacted **1** in the reaction (Figure S6).

Computational Study. Density functional theory (DFT) calculations were also carried out in support of the proposed

mechanism by modeling the isomerization reaction of 1-butene using the Pd(II)–diimine catalyst. Evidently, the activation energy of uncatalyzed 1-butene isomerization in the gas phase is 339 kJ/mol. The activation energy is high, and the reaction is not feasible under the reaction conditions at a relatively low temperature without the assistance of a catalyst. It is further implied that the catalyst requires “activation” for olefin isomerization as the test calculation shows that the coordination of 1-butene to the saturated Pd center is improbable, which disproves the hypothesis of a five-coordinate intermediate. Therefore, the energies required for breaking Pd–N, Pd–Cl, and Pd–C were calculated, and the result supports our proposed pathway by confirming that the dissociation of the Pd–N bond requires the least amount of energy (49.8 kJ/mol). On the other hand, the required energy levels for cleaving Pd–Cl or Pd–C bonds are considerably higher at 343.6 and 183.4 kJ/mol, respectively (Figure S35). It is noted that the calculations do not account for solvent effects, therefore limiting the conclusion to circumstances with weak solvent effects.

Figure 6, top panel, shows the calculated potential energy diagram for 1-butene isomerization beginning with the ligand

dissociation of the initial Pd(II)–diimine catalyst by the Pd–N bond scission with a reaction energy of 49.8 kJ/mol. Following the coordination of 1-butene, the 2,1-insertion has a relatively high activation energy of 105.6 kJ/mol, which aligns with the observed slow insertion rate of the methyl group into the olefin. Notably, this activation energy is lower than that (185.1 kJ/mol) of the methyl insertion without any ligand dissociation. The subsequent β -hydride elimination of the Pd–alkyl complex has a lower activation energy of 64.8 kJ/mol, which results in the internal olefin-complexed Pd–hydride intermediate. The final dissociation of the newly formed internal olefin, followed by the ligand association, has an energy barrier of 19.8 kJ/mol. Based on the calculated energy values, the proposed mechanism appears to be feasible. Subsequent catalytic cycles are catalyzed by the Pd–hydride species, which is compared to the Pd–alkyl pathway in the lower panel of Figure 6. Overall, the isomerization proceeds more easily on Pd–hydride as the energy barriers for most steps are lower in comparison to those for Pd–alkyl species. For instance, the reaction energy for the ligand dissociation of the Pd–hydride catalytic species is 47.9 and 6.8 kJ/mol lower than for Pd–alkyl. More importantly, the 2,1-insertion of this complex with 1-butene has a significantly lower activation energy of only 13.8 kJ/mol, while the following β -hydride elimination has an activation energy of 50.3 kJ/mol. Finally, the successive N-ligand association and 2-butene dissociation to regenerate the catalytic species have an energy barrier of 21.9 kJ/mol. Moreover, the DFT results also help elucidate the influence of diimine ligands' structures on the reaction rate (Figure 7). For the traditional polymerization catalyst C1, the

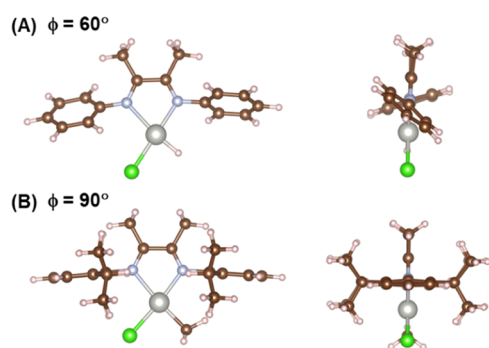


Figure 7. (A) Dihedral angle of 60° for a complex with no aryl *o*-substituent. (B) A dihedral angle of 90° for a complex with isopropyl *o*-substituents.

dihedral angle of the aryl group and the planar Pd(N=C–C=N) backbone is approximately 90° due to the distortion from isopropyl substituents' axial steric bulk. On the other hand, catalysts with no *o*-aryl substituents, such as C3, have a dihedral angle between the aryl group and the planar catalyst backbone of approximately 60°, which is the more favorable conformation. This interpretation infers that the catalysts with more axial steric bulk are more susceptible to ligand dissociation and also more likely to resist ligand's ring closure, which results in better catalytic activity. Hence, C1 performs better than C2 and C3, although its ligand was designed specifically to retard chain transfer, which is key to olefin isomerization theoretically. However, C3 is notably a better isomerization catalyst than C2 experimentally despite having no aryl substitution, which indicates that the catalyst activity is

not solely dependent on the steric effects and that electronic effects should also be taken into account.

Scope of Reaction. While these neutral Pd(II)–diimine complexes exhibit good catalytic activity, the reaction's substrate scope is mainly limited to α -olefins, most likely due to the observed low catalytic efficiency. However, the efficiency improves significantly by using the catalyst in tandem with phenyl silane (PhSiH₃), which has previously been used to generate active Pd–hydride species *via* a Pd–silyl intermediate for olefin isomerization.^{45,46} Specifically, it is proposed that C1 is “activated” by phenyl silane to generate the neutral Pd–silyl intermediate while releasing CH₄ as the byproduct, in which silyl migration into olefin is considerably faster than the methyl analogue (Figure S7).⁴⁷ Hence, the substrate scope expands to various substituted α -olefins, functionalized olefins, and dienes. The isomerization result is summarized in Table 2, as the

Table 2. Substrate Scope for the Palladium-Catalyzed Olefin Isomerization Using Neutral Complex C1

Entry ^[a]	Substrate	Product	Yield(%) ^[b]	<i>E/Z</i> ^[b]
1			80%	5:1
2			99%	3.5:1
3			90%	1.8:1
4			99%	-
5			99%	3.5:1
6			99%	2.4:1
7			99%	11.7:1
8			86% ^[c]	1.7:1
9			84%	15:1
10			91%	-

^aReaction conditions: 0.02 mmol of catalyst C1, 0.06 mmol of PhSiH₃, 0.2 mmol of 1-hexene, 3 mL of dichloromethane at 25 °C.

^bYields and *E/Z* ratios were both calculated using ¹H NMR. Aliquots were taken after 4 h and quenched with Et₃SiH for further analysis.

^cThe aliquot was taken after 16 h.

reactions were carried out using complex C1 and PhSiH₃ with a catalyst loading of 1 and 3 mol %, respectively. Overall, most substrates can be isomerized with high conversion (≥84%) in 4 h. Particularly, the isomerization of various substrates including 5-hexene-2-one, methylenecyclohexane, 1,2-epoxy-5-hexene, tert-butyl(pent-4-en-1-yloxy)silane, and 1-(boc-amino-3-butene) all shows quantitative yield (≥99%). Moreover, the reaction exhibits great regioselectivity for 2-olefins but not stereoselectivity, in which *cis/trans* mixtures were

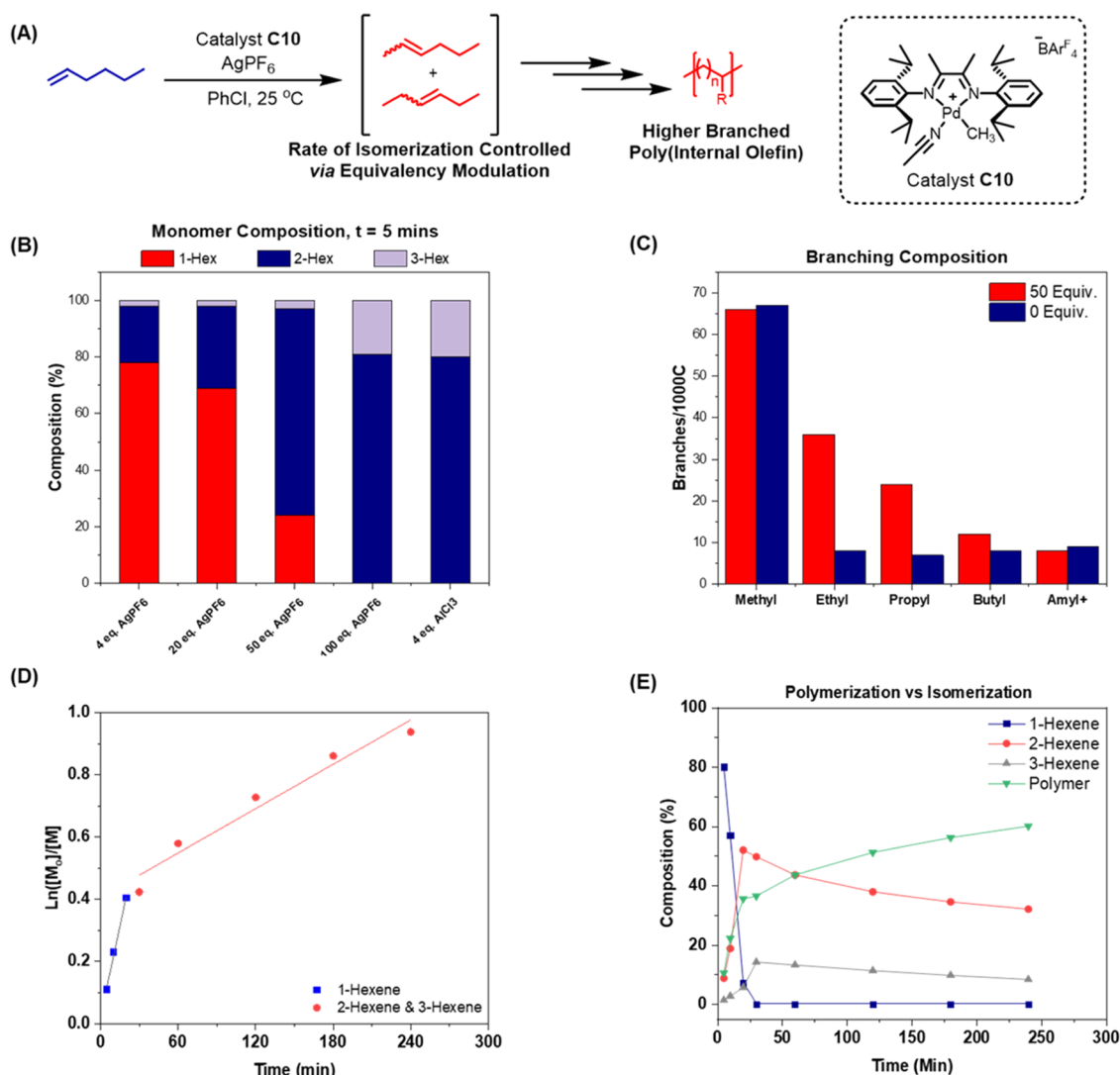


Figure 8. (A) Silver-triggered olefin isomerization-polymerization using catalyst **C10** and AgPF₆. (B) Monomer composition at $t = 5$ min with different equivalents of AgPF₆ in comparison with 4 equiv of AlCl₃. (C) Poly(hexene)'s branching numbers per 1000 carbons calculated via ¹H NMR in the presence of 0 and 50 equiv of AgPF₆. (D) First-order kinetics of the two distinct phases of the reaction in the presence of 4 equiv of AgPF₆. (E) Reaction composition over 4 h calculated via ¹H NMR.

mostly observed. It is notable that 1-hexene isomerization results in only 80% of 2-hexene, while the remaining 20% is 3-hexene. For 1,7-octadiene, only 40% was fully isomerized to 2,6-octadiene, while the other 40% was only partially isomerized to 1,6-octadiene in 4 h. However, the final product mixture improves to 86% of 2,6-octadiene and 14% of 1,6-octadiene after 16 h. Most importantly, this newly discovered catalytic activity of the neutral Pd(II)–diimine catalyst lays the key foundation for the further mechanistic investigation of the paradoxical phenomenon of olefin isomerization-polymerization.

Part 2: Mechanistic Investigation into Olefin Isomerization-Polymerization. As mentioned earlier, olefin isomerization-polymerization behavior is greatly enhanced in the presence of strong Lewis acids such as AlCl₃. However, it is difficult to fully characterize the two simultaneous pathways because the isomerization of α -olefin is completed rapidly in less than 5 min, followed by polymerization of the generated internal olefins. As a result, considerably weaker Lewis acids such AgX (X = [PF₆]⁻, [BF₄]⁻) were tested to evaluate if the

rate of olefin isomerization can be tuned *via* the strength of the Lewis acid, thus offering a better reaction's timeframe for better mechanistic insights into the interrelationship between the two pathways of α -olefin isomerization and polymerization (Figure 8A).

Indeed, the new system of AgX and catalyst **C10** can extend the isomerization window from 5 min up to 30 min, depending on the number of equivalents added. Specifically, optimization of the reaction shows little differences between AgBF₄ and AgPF₆, and the isomerization-polymerization rate is directly proportional to the equivalents of AgX as it increases from 0 up to 100 equiv. Olefin isomerization is inherently observed with less than 10% of 1-hexene readily isomerized to 2-hexene and 3-hexene within the first 5 min when only **C10** is present and 0 equiv of AgPF₆ is used. The rates of isomerization in 5 min improve slowly to 22 and 32% for 4 and 20 equiv of AgPF₆, respectively. When increased to 50 equiv, the conversion increases greatly to 80%, and it finally reaches 100% conversion from 1-hexene to 2-hexene and 3-hexene at 100 equiv of AgPF₆, which is comparable to the result when 4 equiv of AlCl₃

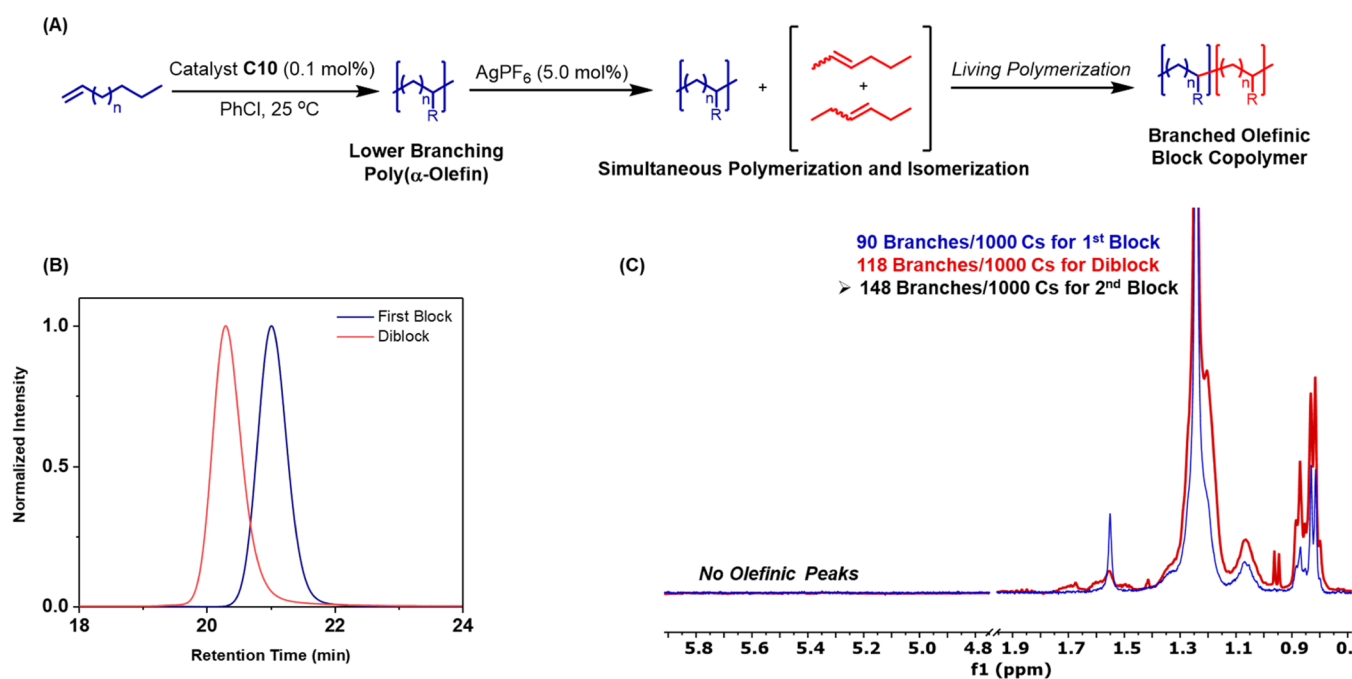


Figure 9. (A) Synthesis of the olefinic block copolymer via silver-triggered olefin isomerization-polymerization. (B) GPC trace for the extended block. (C) ^1H NMR of the final block copolymer showing the branching increase as well as no olefinic peak signal.

is used (Figure 8B). Expectedly, newly formed internal olefins are subsequently polymerized to a high conversion to yield polyolefin with an increased branching number. Particularly, the increase in the number of branching is evident via ^1H NMR as poly(2-hexene-*co*-3-hexene) synthesized after the isomerization in the presence of AgPF_6 (50 equiv) has 150 branches per 1000 carbons, while poly(1-hexene) synthesized without the triggered isomerization from any Lewis acid only has 105 branches per 1000 carbons. Quantitative ^{13}C NMR spectra also offer important insights into the different branching structures of the two polymers. Specifically, poly(hexene) synthesized with 0 equiv of AgPF_6 mainly has methyl branches at 67 branches/1000 carbons, while there are less than 10 branches/1000 carbons for each of ethyl, propyl, butyl, or long branches ($>\text{C}_4$). On the other hand, poly(hexene) synthesized using the new catalyst system has a similar number of methyl branches at 65 branches/1000 carbons, but there are noticeable increases across the board for longer alkyl branches (Figure 8C).

Kinetic studies show that the subsequent polymerization of the newly generated internal olefin remains highly living up to at least 4 h as evidenced by first-order kinetics as well as the constantly narrow molecular weight distributions (MWD) ($M_w/M_n < 1.07$) (Figures S9 and S10). The rate of polymerization is also highly dependent on the equivalents of AgPF_6 used as the first-order rate constant increases approximately 4.5 times from $k = 4.6 \times 10^{-2} \text{ s}^{-1}$ with 4 equiv of AgPF_6 to $k = 2.1 \times 10^{-1} \text{ s}^{-1}$ with 50 equiv of AgPF_6 (Figure S12). More importantly, when only 4 equiv of AgPF_6 were used, it is possible to observe that both the isomerization and polymerization of 1-hexene occur simultaneously until the 1-hexene is fully consumed, which is then followed by the polymerization of the newly formed internal olefin. Specifically, the kinetics demonstrate a clear decrease in the rate of polymerization after 30 min, which is expected, given that internal olefins are harder to polymerize due to their increased steric bulk at the double bond. Additionally, the polymer-

ization vs isomerization data clearly indicate that only α -olefin is consumed *via* either isomerization or polymerization in the first 30 min, and further polymerization of internal olefin does not start until all of the α -olefins are exhausted (Figure 8D,E). Surprisingly, first-order kinetics of both phases suggest that living polymerization is achieved throughout the reaction. The traces in the GPC chromatogram also display a complete shift to higher molecular weights as well as the retention of narrow MWD, which further indicates the lack of chain transfer (Figure S11).

Consequently, this observation would indicate that two different catalyst species are to account for the processes of isomerization and polymerization exclusively. However, the assumption of two present active catalytic species was demonstrated to be incorrect as the olefinic block copolymer (OBC) of α -olefin and internal olefin was successfully synthesized without any observed chain transfer *via* the addition of AgPF_6 halfway through the polymerization. Specifically, 1-hexene was first polymerized by catalyst C10 in 20 min to yield the first block of poly(1-hexene) ($M_n = 9,900$, $M_w/M_n = 1.02$, 90 branches/1000C). Then, 50 equiv of AgPF_6 were added to the reaction, and complete isomerization was observed in less than 10 min. Newly generated 2-hexene and 3-hexene were then polymerized in 30 min to yield poly(1-hexene)-*b*-poly(2-hexene-*co*-3-hexene) ($M_n = 19,000$, $M_w/M_n = 1.02$, 118 branches/1000C) (Figure 9A). From here, the branching number for the second block is calculated to be 148 branches/1000C (SI Section S8, Figure 9C), which is in good agreement with the branching number of poly(2-hexene-*co*-3-hexene). As the first block is living, all of the poly(1-hexene) chains should remain attached to the Pd center upon the addition of AgPF_6 , which then triggers rapid isomerization within 10 min and logically should lead to a considerable amount of chain transfer or dead polymer chains. Therefore, the chain extension efficiency from poly(1-hexene) to poly(1-hexene)-*b*-poly(2-hexene-*co*-3-hexene) should be considerably less than 100%. However, the traces in the GPC chromatogram

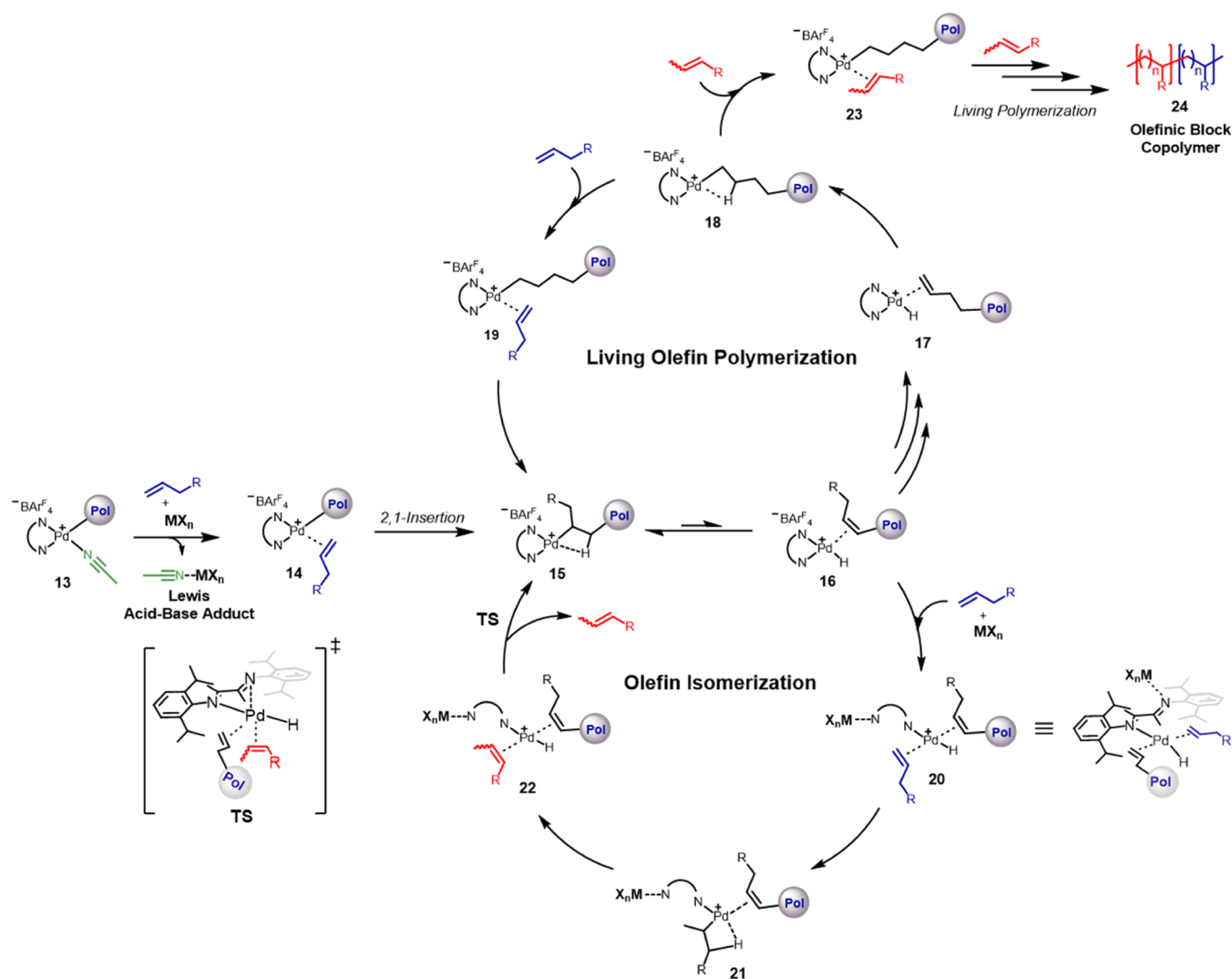


Figure 10. Proposed mechanism for Lewis acid-triggered olefin isomerization-polymerization with simultaneous cycles of olefin isomerization and living polymerization.

still demonstrate a complete shift to higher molecular weights with narrow MWDs (Figure 9B). ^1H NMR spectra of the purified polymer also do not show any vinyl peaks indicative of chain transfer in the 5.5 ppm region, which strongly suggests the quantitative chain extension from the living first block as well as the presence of a single active catalytic species (Figure 9C). As a result, the processes of olefin isomerization and polymerization have to occur simultaneously and independently without chain transfer.

Mechanistic Rationale. In theory, living polymerization of α -olefin is fully expected given the design of C10, which greatly inhibits the process of chain transfer. On the other hand, olefin isomerization is more favorable when chain transfer is promoted. As a result, concurrent olefin isomerization and polymerization should be considered a paradox, and a new mechanistic consideration is necessary to fully explain the two simultaneous and independent catalytic cycles of olefin isomerization and living olefin polymerization using the Pd(II)–diimine catalyst. As the possibilities of chain transfer and two different catalyst species are to be ruled out due to experimental data, which include first-order kinetics, GPC, and NMR results, it would be then postulated that two reactive coordination sites are required on catalyst C10 to satisfy the

two reaction conditions: (1) simultaneous occurrences of olefin isomerization and polymerization, and (2) fully living polymerization with no chain transfer. Evidently, C10 has one inherently open coordination site, which would favor olefin polymerization over isomerization, especially in the absence of a Lewis acid. The second coordination site can thus be accessible *via* the dissociation of one N-ligand of the bidentate diimine, which has been proposed to be a key mechanistic step for olefin isomerization, as discussed earlier in Part 1. The experimental result further supports this proposal, as the presence of a Lewis acid accelerates the isomerization. Particularly, these Lewis acids can outcompete the Pd(II) and coordinate with the N-ligand more strongly, thus assisting the ligand dissociation step. This correlates to the observation that 4 equiv of AlCl_3 have an effect similar to that of 100 equiv of AgPF_6 because AlCl_3 is a much stronger Lewis acid than Pd(II), while Ag(I) and Pd(II) are relatively comparable.

Proposed Mechanism. As a result, a mechanism for Lewis acid-triggered olefin isomerization-polymerization is proposed as follows (Figure 10). The Lewis acid first sequesters MeCN from the domain species 13 by forming a Lewis acid–base adduct to eliminate MeCN's competitive binding against the olefin, which is especially important to the subsequent

polymerization of the generated internal olefin in the later stage of the reaction. α -Olefin then coordinates to the metal center freely to form intermediate **14**, which then undergoes 2,1-migratory insertion and β -hydride elimination to obtain intermediate **15** and **16**, respectively. However, the $\text{Pd}(\text{sec-alkyl})^+$ intermediate like **15** cannot undergo α -olefin insertion, so Pd would have to chain-walk all the way to the polymer chain's terminal end to achieve the $\text{Pd}(n\text{-alkyl})^+$ intermediate **18**.²⁶ The primary Pd–alkyl bond enables the consequential insertion of α -olefin from intermediate **19**, which results in another $\text{Pd}(\text{sec-alkyl})^+$ intermediate **15**, so the Pd would have to chain-walk to the terminal end once again for the next olefin insertion. Additionally, due to the increased steric bulk of α -olefin relative to ethylene, the insertion rate of α -olefin into the primary Pd–alkyl bond would be considerably slower. Moreover, the dissociation rate of α -olefin from the Pd–alkyl complex is also faster, which means that for every cycle of α -olefin insertion into the polymer chain, the Pd would chain-walk over as many as 1000 carbons. Simultaneously, as the Pd chain walks continuously over the polymer chain, multiple catalytic cycles of olefin isomerization could be completed. Specifically, from intermediate **16**, N-ligand dissociation can occur *via* assisted coordination of the Lewis acid to open up on coordination for α -olefin, which results in intermediate **20**. As discussed above, chain transfer is not observed, which indicates that the olefinic polymer species does not undergo ligand displacement at any given step. Hence, it is proposed that the dissociated N-ligand would remain close to the Pd center due to the chelate effect and that this intermediate would partially retain the complex's original conformation, in which the dissociated diimine ligand still offers adequate axial steric bulk to prevent the further axial attack of α -olefin. From here, the α -olefin would insert into the Pd–hydride bond instead, which temporarily halts the chain-walking process of the polymer to form intermediate **21**. It then undergoes β -hydride elimination to obtain the complexed internal olefin intermediate **22**, and the isomerized internal olefin would then be displaced *via* N-ligand association from the axial position while the polymer chain swiftly reinserts into the Pd–hydride bond to regenerate **15**. Specifically for the transition state, the axial approach of the N-ligand association forces the intermediate's geometry from square planar to trigonal bipyramidal, in which the internal olefin is forced to the axial position and then dissociates. Particularly, the shift of the considerably smaller internal olefin from planar to the axial position is inferred to be more favorable than that of the bulky unsaturated polymer chain due to the intermediate's retained axial steric bulk. These two simultaneous cycles would continue until the α -olefin is fully consumed either *via* isomerization or polymerization, and the in situ generated internal olefin would then freely coordinate to intermediate **18** and propagate from the same living polymer chain of the resulting intermediate **23** to yield olefinic block copolymer (OBC) **24**. The rate of olefin isomerization can be easily modulated by either employing different weak/strong Lewis acids or regulating the Lewis acid's equivalents, which results in different compositions for the block copolymer.

Finally, the increase in branching numbers between poly(α -olefin) and poly(internal olefin) is most likely accounted by the different enchainments between α -olefin and internal olefin and not the potentially increased chain-walking rate arising from the elimination of MeCN's competitive binding. This aligns well with the branching profiles of both poly(1-hexene) and poly(2-hexene-*co*-3-hexene). For example, α -olefin favors

1,2- and 2,1-insertion about equally, in which 2,1-insertion results in ω ,1 enchainment or chain-straightened segment, and 1,2-insertion primarily leads to ω ,2-enchainment or methyl branches. On the other hand, internal olefins such as 2-hexene can produce either ω ,2-enchainment/methyl branches from 3,2-insertion or 1,3-enchainment/longer alkyl branches from 2,3 insertion and further chain-walking (Figure 11).^{26,27}

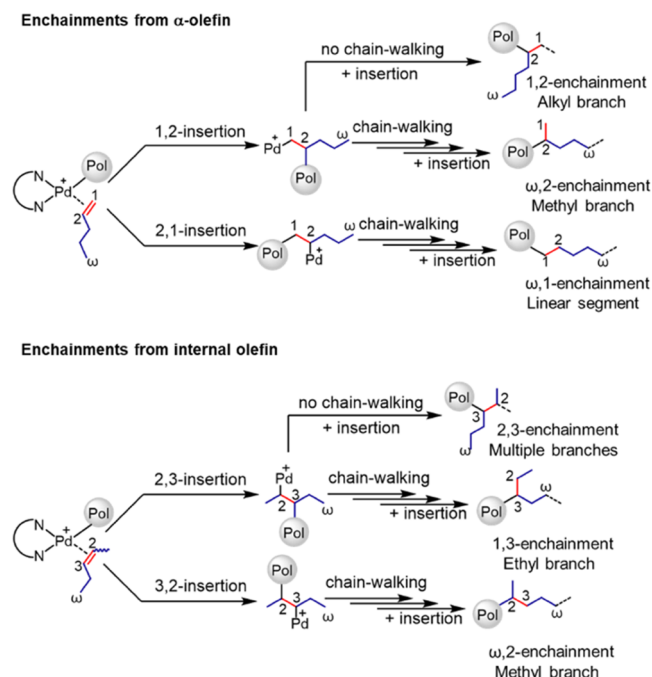


Figure 11. Branching resulted from different enchainments of α -olefins and internal olefins.

Notably, poly(1-hexene) still has a small number of ethyl and longer alkyl branches due to a small incorporation of both 2-hexene and 3-hexene generated from the isomerization, even in the absence of a Lewis acid. Additionally, ethylene polymerization using the same system shows only an increase in the molecular weight but no difference in the branching numbers, which indicates ethylene's obvious inability to isomerize as well as no influence on the chain-walking rate in the absence of the competitive ancillary ligand (Figures S32 and S33). In fact, the presence of MeCN has been shown to induce the opposite effect on ethylene polymerization as an increased amount leads to faster chain-walking and thus a higher branching level.⁴⁸

Part 3: Photoinitiated Switch from Olefin Isomerization-Polymerization to MILRad Polymerization: The Synthesis of the Polyolefin-Polar Block Copolymer. The demonstrated livingness of Lewis acid-triggered olefin isomerization-polymerization is important because it helps in elucidating the newly proposed mechanistic pathway as well as the switchability of the well-studied Pd(II)–diimine catalyst. More interestingly, the living polymerization is also crucial for the transition from the insertion pathway of Lewis acid-triggered olefin isomerization-polymerization to the radical pathway of MILRad polymerization to further synthesize block copolymers of olefin and acrylate in a one-pot synthesis. Specifically, the key step of MILRad polymerization is the formation of a stable six-member macrocholate upon the insertion of one acrylate monomer. The macrocholate then

undergoes the process of ring-opening and homolytic Pd–C bond cleavage of the polymer chain from the metal center *via* light irradiation.³³ Thus, the livingness of the insertion pathway would guarantee the quantitative generation of the radical macroinitiator for the subsequent free radical polymerization (Figure 12).^{33,49} However, the transition from the insertion to

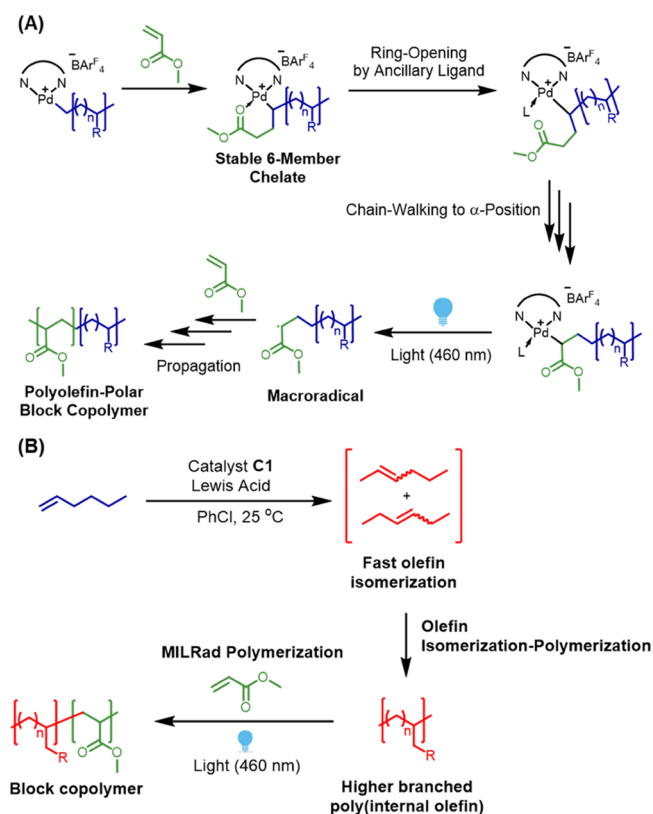


Figure 12. (A) Key mechanistic steps of MILRad polymerization. (B) The transition from Lewis acid-triggered olefin isomerization-polymerization to MILRad polymerization.

the radical pathway of MILRad proves to be not straightforward as various Lewis acids exhibit little compatibility toward free radical polymerization. Particularly, the presence of AlCl_3 completely inhibits the free radical pathway of MILRad polymerization as chain extension of poly(hexene) with poly(methyl acrylate) is not observed after the switch to the light cycle. The negative influence of AlCl_3 on free radical polymerization is further corroborated by studies done by Brumby et al., which demonstrated the retardation of free radical polymerization of methyl acrylate using AIBN in the presence of AlCl_3 .⁵⁰ Additional Lewis acids, including TiCl_4 , ZnCl_2 , and FeCl_3 , were then investigated but showed mixed results (SI Section S5). Similar to AlCl_3 , TiCl_4 and FeCl_3 can trigger olefin isomerization but completely inhibit free radical polymerization. On the other hand, ZnCl_2 works for both pathways, but the rate of isomerization for ZnCl_2 (and FeCl_3) is slow even at high equivalents (up to 50 equiv), which can be attributed to the poor solubility in organic solvents as well as lower Lewis acidity compared to that of AlCl_3 . Consequently, Ag(I) Lewis acids such as AgBF_4 and AgPF_6 were chosen as they have superior solubility in organic solvents, and more importantly, Matyjaszewski et al. have previously reported that neither the presence of Ag(0) nor Ag(I) retarded free radical polymerization.⁵¹ Indeed, AgX ($\text{X} = [\text{BF}_4]^-$, $[\text{PF}_6]^-$) in tandem with catalyst C10 is capable of initiating MILRad polymerization to synthesize polyolefin-polar block copolymers.

Sequential One-Pot Synthesis of the Polyolefin-Acrylate Block Copolymer with Varied Composition. The catalyst system of C10 and AgPF_6 was used to synthesize the diblock copolymer of internal hexenes and methyl acrylate. 1-Hexene was first polymerized by catalyst C10 in the presence of 50 equiv of AgPF_6 to obtain highly branched poly(2-hexene-*co*-3-hexene) ($M_n = 17,200$, $M_w/M_n = 1.03$, 146 branches/1000C). Methyl acrylate was swiftly added, and the reaction was irradiated under blue light ($\lambda = 460$ nm) for 4 h to yield diblock poly(2-hexene-*co*-3-hexene)-*b*-poly(methyl acrylate) ($M_n = 111,000$, $M_w/M_n = 1.44$), which demonstrated the successful combination of the two techniques for the first time. Ultimately, this result allows for the further synthesis of new

Table 3. α -Olefins/Acrylate Block Copolymerization

Reaction scheme for Table 3:

1-olefin + Catalyst **C10** (0.1 mol%) in PhCl, 25 °C → Lower Branching Polymer

Lower Branching Polymer + AgPF₆ (5.0 mol%) → Branched Block Copolymer

Branched Block Copolymer + Acrylate (CH₂=CH-C(=O)OR) under Light (460 nm) → Polyolefin-Acrylate Block Copolymer

Table 3. Synthesis of polyolefin-acrylate triblock copolymers by the sequential addition of AgPF₆ and acrylates to the lower branching polymer prepared by catalyst **C10** in PhCl at 25 °C. ^a Entry numbers are the same as in Table 1. ^b Acrylates were added to the lower branching polymer in PhCl at 25 °C. ^c The molecular weights were determined by GPC with a refractive index detector. ^d The number of branches per 1000 carbon atoms was determined by ¹³C NMR. ^e The melting and glass transition temperatures were determined by DSC. ^f The molecular weight of the lower branching polymer was determined by GPC with a refractive index detector.

entry ^a	olefin	acrylate ^b	1st block			diblock		triblock			incorp ^d (mol %)	<i>T</i> _m ^e (°C)	<i>T</i> _g ^e (°C)	<i>T</i> _g ^{e'} (°C)
			<i>M</i> _n ^c (g/mol)	<i>M</i> _w / <i>M</i> _n ^c	branches 1000C ^d	<i>M</i> _n ^c (g/mol)	<i>M</i> _w / <i>M</i> _n ^c	branches 1000C ^d	<i>M</i> _n ^c (g/mol)	<i>M</i> _w / <i>M</i> _n ^c				
1	1-hexene	MA	14,000	1.01	90	20,000	1.02	118	97,000	1.64	78%			9
2	1-hexene	<i>n</i> BA	12,000	1.02	85	19,000	1.02	115	93,000	1.41	75%			−51
3	1-hexene	MMA	12,000	1.02	96	20,000	1.02	116	93,000	2.15	52%			108
4	1-decene	MA	28,000	1.03	65	36,000	1.05	76	160,000	1.66	75%	46	−72	9
5 ^f	1-odadecene	MA	8500	1.10	34	17,000	1.10	71	141,000	1.66	81%	78	−26	10

^aReaction conditions: 0.02 mmol of catalyst **1**, 1 mmol (50 equiv.) of AgPF_6 , 6 mL of chlorobenzene (PhCl), 25 °C. Twenty minutes for the 1st block, 30 min for the second block, and 4 h for 3rd block. The monomer ratio [Cat/Olefin/Acrylate] for **1** is [1:800:1100], **2** is [1:800:700], **3** is [1:800:940], **4** is [1:530:1100], and **5** is [1:310:1100]. ^bAbbreviations: methyl acrylate (MA), *n*-butyl acrylate (nBA), and methyl methacrylate (MMA). ^cDetermined by gel permeation chromatography (GPC) in THF at 40 °C calibrated to polystyrene standards. ^dDetermined by ¹H NMR in CDCl_3 at 25 °C. ^eDetermined by differential calorimetry scanning (DSC). ^fMolecular weight was determined by GPC in trichlorobenzene (TCB) at 150 °C.

triblock copolymers whose motif includes a lower-branched polyolefin first block, a higher-branched polyolefin second block, and a polyacrylate third block. Similar to the previous diblock syntheses, poly(1-hexene)-*b*-poly(2-hexene-*co*-3-hexene) was synthesized using catalyst **C10** with the addition of AgPF₆ (50 equiv.) halfway through the polymerization with a monomer conversion of 25 and 43%, respectively, after the formation of each block. Subsequently, methyl acrylate was introduced as the reaction was irradiated under blue light for 4 h to give the final poly(1-hexene)-*b*-poly(2-hexene-*co*-3-hexene)-*b*-poly(methyl acrylate) (Table 3, entry 1). Different block copolymers were also successfully synthesized using various α -olefins as well as acrylates such as methyl methacrylate and *n*-butyl acrylate, as summarized in Table 3. Similar to the previous synthesis, the first two blocks of poly(hexene) were targeted at approximately 20,000 g/mol, which was subsequently followed by the polymerization of methyl methacrylate and *n*-butyl acrylate in 4 h to yield poly(1-hexene)-*b*-poly(2-hexene-*co*-3-hexene)-*b*-poly(methyl methacrylate) (Table 3, entry 3) and poly(1-hexene)-*b*-poly(2-hexene-*co*-3-hexene)-*b*-poly(*n*-butyl acrylate) (Table 3, entry 2), respectively. In comparison to methyl acrylate, the polymerization result for *n*-butyl acrylate was relatively comparable, which was reflected by the similar polydispersity as well as the high monomer incorporation. Specifically, poly(1-hexene)-*b*-poly(2-hexene-*co*-3-hexene)-*b*-poly(*n*-butyl acrylate) showed high incorporation of 75% for *n*-butyl acrylate after 4 h compared to the incorporation of 78% for methyl acrylate. On the other hand, the polymerization of methyl methacrylate was not as controlled as the molecular weight distribution was especially broad, and the monomer incorporation was only 55% compared to those of methyl acrylate and *n*-butyl acrylate. Additionally, longer α -olefins such as 1-decene and 1-octadecene were also used to demonstrate the ability to synthesize OBCs consisting of both semi-crystalline and amorphous segments. Specifically, poly(1-decene)-*b*-poly(2-decene)-*b*-poly(methyl acrylate) (Table 3, entry 4) exhibits a T_m of 46 °C for the poly(1-decene) segment and two different T_g of -72 and 9 °C for the amorphous poly(2-decene) and poly(methyl acrylate) segments, respectively. Similarly, poly(1-octadecene)-*b*-poly(2-octadecene)-*b*-poly(methyl acrylate) (Table 3, entry 5) also displays a moderately high T_m of 78 °C for the semi-crystalline poly(1-octadecene) segment, while the other two amorphous segments of poly(2-octadecene) and poly(methyl acrylate) have their respective T_g at -26 and 10 °C. Other characterization methods, including diffusion-ordered spectroscopy (DOSY) and small-angle X-ray scattering (SAXS), are also used to confirm the block copolymer structures. For instance, the ¹H DOSY NMR spectrum of poly(1-hexene)-*b*-poly(2-hexene-*co*-3-hexene)-*b*-poly(methyl acrylate) (Table 3, entry 1) shows that all of the corresponding peaks of poly(hexene) and poly(methyl acrylate) populate around a single diffusion coefficient, which indicates that the two blocks are covalently bonded. Additionally, the SAXS profile reveals a principle scattering peak, which is evident of microphase separation on the order of 110 nm of the two immiscible olefin and acrylate blocks (Figure 13). Higher-order peaks also show long-range order, which is consistent with a lamellar structure.

Architectural Model of Block Copolymers. However, it should be considered that the OBC does not follow the typical linear AB motif. As discussed earlier, Pd can chain-walk up to 1000 carbons before one α -olefin/internal olefin inserts into

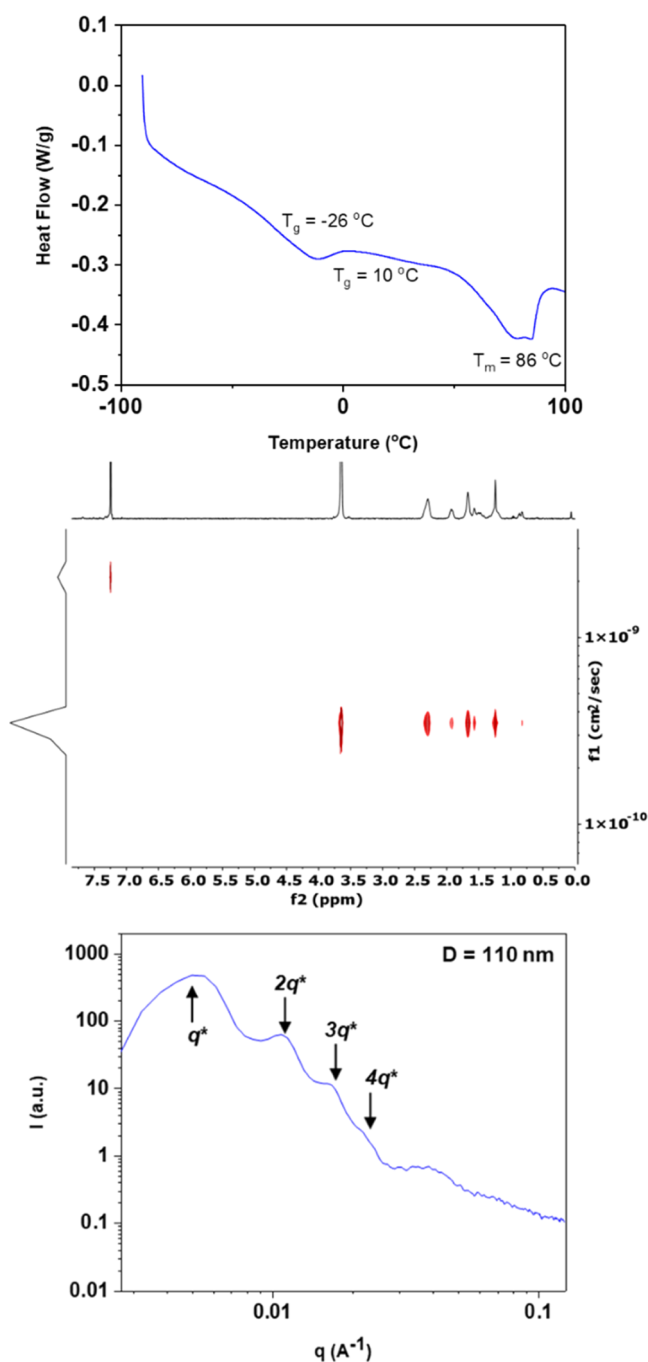


Figure 13. (Top) DSC of poly(1-octadecene)-*b*-poly(2-octadecene)-*b*-poly(methyl acrylate) (Table 3, entry 5); (middle) ¹H DOSY of poly(1-hexene)-*b*-poly(2-hexene-*co*-3-hexene)-*b*-poly(methyl acrylate) (Table 3, entry 1); and (bottom) SAXS of poly(1-hexene)-*b*-poly(2-hexene-*co*-3-hexene)-*b*-poly(methyl acrylate) (Table 3, entry 1).

the primary Pd(*n*-alkyl⁺) complex, which means that Pd will have to chain-walk all the way to one of the branches' ends between each olefin insertion. As a result, Brookhart et al. proposed the microstructure model for the diblock to be a "core-shell" structure such that the first block of lower-branched polyolefin acts as the main backbone, while the second highly branched polyolefin block would propagate from different ends of the first block's branches to form numerous segments surrounding the backbone.²⁶ However, while the proposed core-shell architecture is reasonably supported by

theory, the experimental data suggest that there might be a discrepancy between the proposed model and the actual correct architectures. Characteristically, both poly(1-octadecene)-*b*-poly(2-octadecene) and poly(1-decene)-*b*-poly(2-decene) still exhibit T_m from the semi-crystalline “core” of poly(1-octadecene) and poly(1-decene) as shown above, which contradicts the idea of a core–shell structure because the core should lose its crystalline characteristics due to the increasing long chain “branching” of the shell. However, while OBC’s architecture should still realistically follow Brookhart’s proposed model due to the established chain-walking behavior, the number and density of the shell segments should be much lower than predicted. Finally, the third and final block will grow from a single chain end. Upon the addition of methyl acrylate, the polyolefin diblock is end-capped at one branch end of either the first or second block, and a stable 6-member chelate is formed, which then undergoes Pd–C bond cleavage under irradiation of light to initiate MILRad polymerization. As a result, the final block copolymer can be considered to be a mixture of two slightly different triblock copolymers (Figure 14).

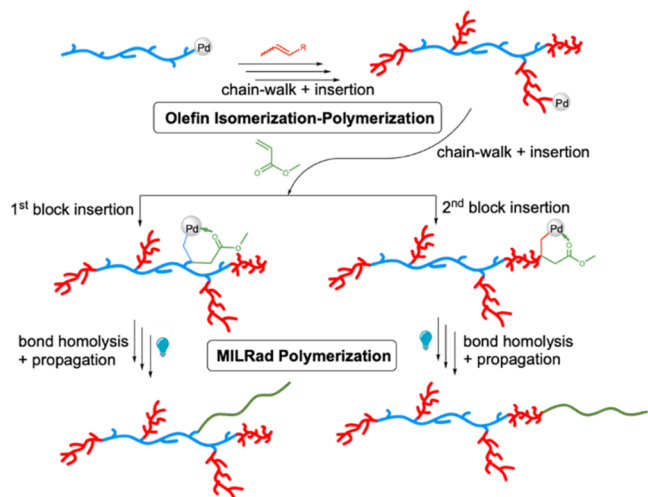


Figure 14. Proposed model for the growth of polyolefin-acrylate block copolymers.

Further mechanical testing was carried out using poly(decene)-based polymers to study the potential correlations between these block copolymers’ microstructures and their macroscopic properties (Figures 15 and S31). Specifically, poly(1-decene), whose T_m was detected at 46 °C, exhibits behaviors of soft and ductile plastic with a modulus of 17.0 MPa and a maximum elongation of 41% before breaking. Interestingly, the poly(1-decene)-*b*-poly(2-decene) diblock with the incorporation of the higher-branched polymer arms becomes a softer yet significantly more brittle polymer in comparison to poly(1-decene) as it has a linear stress–strain curve with a modulus of 2.6 MPa and minimal elongation at a break of 5.4%. However, the poly(1-decene)-*b*-poly(2-decene)-*b*-poly(methyl acrylate) triblock exhibits elastomeric characteristics due to its extremely low modulus of 1.3 MPa as well as its high stretchability with a maximum strain of 310%. The behavior can be attributed to the introduction of the amorphous yet tough poly(methyl acrylate) block, whose T_g is detected at 10 °C (Figure S29D).

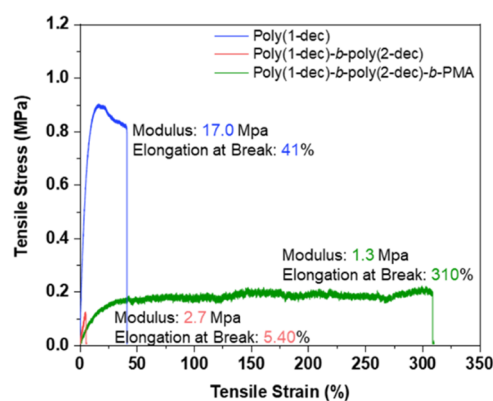


Figure 15. Tensile testing of poly(1-decene) and poly(decene)-based block copolymers.

CONCLUSIONS

In summary, we offer a novel insight into a long-standing paradox in which isomerization and living polymerization are simultaneously observed in Pd-catalyzed α -olefin polymerization. This experimental observation remains questionable, given the current mechanistic understanding of these complexes. The study of the unusual palladium-catalyzed α -olefin isomerization using the nonactivated neutral Pd(II)–diimine catalysts, which exhibits moderate to good activity depending on the ligands, reveals a new key mechanistic step involving the dissociation from one “arm” of the bidentate diimine ligand to open up one coordination site for the olefin. This proposal is supported by experimental data and DFT calculations. More importantly, this finding shows that coordination sites in Pd complexes can be generated by ligand dissociation and not catalyst activation exclusively. Experimental studies with activated cationic Pd(II) diimine complexes indicate that a ligand dissociation is also possible to generate the second coordination site that allows for simultaneous isomerization and living polymerization. This mechanistic proposal corroborates with the observed olefin isomerization-polymerization as it explains how two independent catalytic cycles of olefin isomerization and olefin polymerization can occur simultaneously without leading to chain transfer, hence the persistent living polymerization. We propose that while the living polymerization pathway proceeds through the classical mechanism, the isomerization pathway would not compete for the same coordination site but proceed in a similar manner as observed in the α -olefin isomerization by neutral Pd(II)–diimine catalysts. Notably, this mechanistic behavior is also greatly enhanced in the presence of a Lewis acid, given a much higher rate of isomerization due to the accelerated rate of ligand dissociation *via* competitive binding. Finally, we investigated the photoinitiated switch from Lewis acid-triggered olefin isomerization-polymerization to MILRad polymerization, and AgX ($X = [BF_4]^-$, $[PF_6]^-$) are found to be the most compatible Lewis acids toward both methods. Ultimately, various polyolefin-polar block copolymers with unique architectures and distinct levels of branching, crystallinity, and polar functionality were successfully synthesized in an elegant one-pot manner.

ASSOCIATED CONTENT

Supporting Information

The Supporting Information is available free of charge at <https://pubs.acs.org/doi/10.1021/jacs.3c01513>.

Experimental procedures; methods; computation; and characterization of compounds (PDF)

AUTHOR INFORMATION

Corresponding Authors

Lars C. Grabow — Williams A. Brookshire Department of Chemical and Biomolecular Engineering, University of Houston, Houston, Texas 77204, United States; Center for Programmable Energy Catalysis (CPEC), University of Minnesota, Minneapolis, Minnesota 55455, United States; orcid.org/0000-0002-7766-8856; Email: grabow@uh.edu

Eva Harth — Department of Chemistry, Center of Excellence in Polymer Chemistry (CEPC), University of Houston, Houston, Texas 77204, United States; orcid.org/0000-0001-5553-0365; Email: harth@uh.edu

Authors

Dung Nguyen — Department of Chemistry, Center of Excellence in Polymer Chemistry (CEPC), University of Houston, Houston, Texas 77204, United States

Shengguang Wang — Williams A. Brookshire Department of Chemical and Biomolecular Engineering, University of Houston, Houston, Texas 77204, United States; Center for Programmable Energy Catalysis (CPEC), University of Minnesota, Minneapolis, Minnesota 55455, United States

Complete contact information is available at:

<https://pubs.acs.org/10.1021/jacs.3c01513>

Author Contributions

This manuscript was written through contributions of all authors. The authors declare no competing financial interest.

Notes

The authors declare no competing financial interest.

ACKNOWLEDGMENTS

The authors D.N. and E.H. thank the Robert A. Welch Foundation for the generous support of this research (#H-E-0041 and #E-2066-202110327) through the Center of Excellence in Polymer Chemistry. The computational studies contributed by S.W. and L.C.G. were supported as part of the Center for Programmable Energy Catalysis, an Energy Frontier Research Center funded by the U.S. Department of Energy, Office of Science, Basic Energy Sciences at the University of Minnesota under award #DE-SC0023464. The authors also gratefully acknowledge the National Science Foundation for supporting parts of this work (CHEM-2108576). The authors thank Dr. Steve Swinnea for SAXS measurements at UT Austin and acknowledge the use of the Carya, Opuntia, and Sabine cluster resources provided by the Research Computing Data Core at the University of Houston. The authors thank Ibrahim Kamara from the Robertson Group, UH Chemical Engineering, for assisting with the tensile testing measurements. The authors would also like to acknowledge Dr. Yu-Sheng Liu, formerly a Harth group member, now at Merck Inc., for his valuable and insightful discussions.

REFERENCES

- (1) Johnson, L. K.; Killian, C. M.; Brookhart, M. New Pd(II)- and Ni(II)-Based Catalysts for Polymerization of Ethylene and α -Olefins. *J. Am. Chem. Soc.* **1995**, *117*, 6414–6415.
- (2) Johnson, L. K.; Mecking, S.; Brookhart, M. Copolymerization of Ethylene and Propylene with Functionalized Vinyl Monomers by Palladium(II) Catalysts. *J. Am. Chem. Soc.* **1996**, *118*, 267–268.
- (3) Killian, C. M.; Tempel, D. J.; Johnson, L. K.; Brookhart, M. Living Polymerization of α -Olefins Using NiII- α -Diimine Catalysts. Synthesis of New Block Polymers Based on α -Olefins. *J. Am. Chem. Soc.* **1996**, *118*, 11664–11665.
- (4) Domski, G. J.; Rose, J. M.; Coates, G. W.; Bolig, A. D.; Brookhart, M. Living alkene polymerization: New methods for the precision synthesis of polyolefins. *Prog. Polym. Sci.* **2007**, *32*, 30–92.
- (5) Ittel, S. D.; Johnson, L. K.; Brookhart, M. Late-Metal Catalysts for Ethylene Homo- and Copolymerization. *Chem. Rev.* **2000**, *100*, 1169–1204.
- (6) Brookhart, M.; Green, M. L. H.; Parkin, G. Agostic interactions in transition metal compounds. *Proc. Natl. Acad. Sci. U.S.A.* **2007**, *104*, 6908–6914.
- (7) Leatherman, M. D.; Svejda, S. A.; Johnson, L. K.; Brookhart, M. Mechanistic Studies of Nickel(II) Alkyl Agostic Cations and Alkyl Ethylene Complexes: Investigations of Chain Propagation and Isomerization in (α -diimine)Ni(II)-Catalyzed Ethylene Polymerization. *J. Am. Chem. Soc.* **2003**, *125*, 3068–3081.
- (8) Svejda, S. A.; Johnson, L. K.; Brookhart, M. Low-Temperature Spectroscopic Observation of Chain Growth and Migratory Insertion Barriers in (α -Diimine)Ni(II) Olefin Polymerization Catalysts. *J. Am. Chem. Soc.* **1999**, *121*, 10634–10635.
- (9) Shultz, L. H.; Tempel, D. J.; Brookhart, M. Palladium(II) β -Agostic Alkyl Cations and Alkyl Ethylene Complexes: Investigation of Polymer Chain Isomerization Mechanisms. *J. Am. Chem. Soc.* **2001**, *123*, 11539–11555.
- (10) Deng, L.; Margl, P.; Ziegler, T. A Density Functional Study of Nickel(II) Diimide Catalyzed Polymerization of Ethylene. *J. Am. Chem. Soc.* **1997**, *119*, 1094–1100.
- (11) Deng, L.; Woo, T. K.; Cavallo, L.; Margl, P. M.; Ziegler, T. The Role of Bulky Substituents in Brookhart-Type Ni(II) Diimine Catalyzed Olefin Polymerization: A Combined Density Functional Theory and Molecular Mechanics Study. *J. Am. Chem. Soc.* **1997**, *119*, 6177–6186.
- (12) Michalak, A.; Ziegler, T. Palladium-Catalyzed Polymerization of Propene: DFT Model Studies. *Organometallics* **1999**, *18*, 3998–4004.
- (13) Musaev, D. G.; Froese, R. D. J.; Svensson, M.; Morokuma, K. A Density Functional Study of the Mechanism of the Diimine-Nickel-Catalyzed Ethylene Polymerization Reaction. *J. Am. Chem. Soc.* **1997**, *119*, 367–374.
- (14) Froese, R. D. J.; Musaev, D. G.; Morokuma, K. Theoretical Study of Substituent Effects in the Diimine-M(II) Catalyzed Ethylene Polymerization Reaction Using the IMOMM Method. *J. Am. Chem. Soc.* **1998**, *120*, 1581–1587.
- (15) O'Connor, K. S.; Lamb, J. R.; Vaidya, T.; Keresztes, I.; Klimovica, K.; LaPointe, A. M.; Daugulis, O.; Coates, G. W. Understanding the Insertion Pathways and Chain Walking Mechanisms of α -Diimine Nickel Catalysts for α -Olefin Polymerization: A ^{13}C NMR Spectroscopic Investigation. *Macromolecules* **2017**, *50*, 7010–7027.
- (16) Allen, K. E.; Campos, J.; Daugulis, O.; Brookhart, M. Living Polymerization of Ethylene and Copolymerization of Ethylene/Methyl Acrylate Using “Sandwich” Diimine Palladium Catalysts. *ACS Catal.* **2015**, *5*, 456–464.
- (17) Tran, Q. H.; Brookhart, M.; Daugulis, O. New Neutral Nickel and Palladium Sandwich Catalysts: Synthesis of Ultra-High Molecular Weight Polyethylene (UHMWPE) via Highly Controlled Polymerization and Mechanistic Studies of Chain Propagation. *J. Am. Chem. Soc.* **2020**, *142*, 7198–7206.
- (18) Vaccarello, D. N.; O'Connor, K. S.; Iacono, P.; Rose, J. M.; Cherian, A. E.; Coates, G. W. Synthesis of Semicrystalline Polyolefin Materials: Precision Methyl Branching via Stereoretentive Chain Walking. *J. Am. Chem. Soc.* **2018**, *140*, 6208–6211.
- (19) O'Connor, K. S.; Watts, A.; Vaidya, T.; LaPointe, A. M.; Hillmyer, M. A.; Coates, G. W. Controlled Chain Walking for the

Synthesis of Thermoplastic Polyolefin Elastomers: Synthesis, Structure, and Properties. *Macromolecules* **2016**, *49*, 6743–6751.

(20) Dai, S.; Sui, X.; Chen, C. Highly Robust Palladium(II) α -Diimine Catalysts for Slow-Chain-Walking Polymerization of Ethylene and Copolymerization with Methyl Acrylate. *Angew. Chem., Int. Ed.* **2015**, *54*, 9948–9953.

(21) Dai, S.; Chen, C. Direct Synthesis of Functionalized High-Molecular-Weight Polyethylene by Copolymerization of Ethylene with Polar Monomers. *Angew. Chem., Int. Ed.* **2016**, *55*, 13281–13285.

(22) Zhang, Y.; Wang, C.; Mecking, S.; Jian, Z. Ultrahigh Branching of Main-Chain-Functionalized Polyethylenes by Inverted Insertion Selectivity. *Angew. Chem., Int. Ed.* **2020**, *59*, 14296–14302.

(23) Kenyon, P.; Wörner, M.; Mecking, S. Controlled Polymerization in Polar Solvents to Ultrahigh Molecular Weight Polyethylene. *J. Am. Chem. Soc.* **2018**, *140*, 6685–6689.

(24) Liu, Y.-S.; Harth, E. Distorted Sandwich α -Diimine PdII Catalyst: Linear Polyethylene and Synthesis of Ethylene/Acrylate Elastomers. *Angew. Chem., Int. Ed.* **2021**, *60*, 24107–24115.

(25) Tempel, D. J. Mechanistic Studies of Palladium(II)- and Nickel(II)-Catalyzed Olefin Polymerization. Ph.D. Dissertation, The University of North Carolina at Chapel Hill: Ann Arbor, 1998.

(26) Gottfried, A. C.; Brookhart, M. Living and Block Copolymerization of Ethylene and α -Olefins Using Palladium(II)- α -Diimine Catalysts. *Macromolecules* **2003**, *36*, 3085–3100.

(27) McCord, E. F.; McLain, S. J.; Nelson, L. T. J.; Ittel, S. D.; Tempel, D.; Killian, C. M.; Johnson, L. K.; Brookhart, M. ¹³C NMR Analysis of α -Olefin Enchainment in Poly(α -olefins) Produced with Nickel and Palladium α -Diimine Catalysts. *Macromolecules* **2007**, *40*, 410–420.

(28) Ji, M.; Si, G.; Pan, Y.; Tan, C.; Chen, M. Polymeric α -diimine palladium catalysts for olefin (co)polymerization. *J. Catal.* **2022**, *415*, 51–57.

(29) Dai, S.; Zhou, S.; Zhang, W.; Chen, C. Systematic Investigations of Ligand Steric Effects on α -Diimine Palladium Catalyzed Olefin Polymerization and Copolymerization. *Macromolecules* **2016**, *49*, 8855–8862.

(30) Zhao, M.; Chen, C. Accessing Multiple Catalytically Active States in Redox-Controlled Olefin Polymerization. *ACS Catal.* **2017**, *7*, 7490–7494.

(31) Basbug Alhan, H. E.; Jones, G. R.; Harth, E. Branching Regulation in Olefin Polymerization via Lewis Acid Triggered Isomerization of Monomers. *Angew. Chem., Int. Ed.* **2020**, *59*, 4743–4749.

(32) Jones, G. R.; Basbug Alhan, H. E.; Karas, L. J.; Wu, J. I.; Harth, E. Switching the Reactivity of Palladium Diimines with “Ancillary” Ligand to Select between Olefin Polymerization, Branching Regulation, or Olefin Isomerization. *Angew. Chem., Int. Ed.* **2021**, *60*, 1635–1640.

(33) Keyes, A.; Basbug Alhan, H. E.; Ha, U.; Liu, Y.-S.; Smith, S. K.; Teets, T. S.; Beezer, D. B.; Harth, E. Light as a Catalytic Switch for Block Copolymer Architectures: Metal–Organic Insertion/Light Initiated Radical (MILRad) Polymerization. *Macromolecules* **2018**, *51*, 7224–7232.

(34) Chen, C.; Luo, S.; Jordan, R. F. Multiple Insertion of a Silyl Vinyl Ether by (α -Diimine)PdMe⁺ Species. *J. Am. Chem. Soc.* **2008**, *130*, 12892–12893.

(35) Chen, C.; Jordan, R. F. Palladium-Catalyzed Dimerization of Vinyl Ethers to Acetals. *J. Am. Chem. Soc.* **2010**, *132*, 10254–10255.

(36) Winston, M. S.; Oblad, P. F.; Labinger, J. A.; Bercaw, J. E. Activator-Free Olefin Oligomerization and Isomerization Reactions Catalyzed by an Air- and Water-Tolerant Wacker Oxidation Intermediate. *Angew. Chem., Int. Ed.* **2012**, *51*, 9822–9824.

(37) Tao, W.-J.; Li, J.-F.; Peng, A.-Q.; Sun, X.-L.; Yang, X.-H.; Tang, Y. Water as an Activator for Palladium(II)-Catalyzed Olefin Polymerization. *Chem. - Eur. J.* **2013**, *19*, 13956–13961.

(38) Groen, J. H.; Delis, J. G. P.; van Leeuwen, P. W. N. M.; Vrieze, K. Kinetic Study of the Insertion of Norbornadiene into Palladium–Carbon Bonds of Complexes Containing the Rigid Bidentate

Nitrogen Ligand Bis(arylimino)acenaphthene. *Organometallics* **1997**, *16*, 68–77.

(39) Thorn, D. L.; Hoffmann, R. The olefin insertion reaction. *J. Am. Chem. Soc.* **1978**, *100*, 2079–2090.

(40) Van Leeuwen, P. W. N. M.; Roobeek, C. F.; Frijns, J. H. G.; Orpen, A. G. Characterization of the intermediates in the hydroformylation reaction catalyzed by platinum diphenylphosphinous acid complexes. *Organometallics* **1990**, *9*, 1211–1222.

(41) Clark, H. C.; Jablonski, C.; Halpern, J.; Mantovani, A.; Weil, T. A. Mechanism of insertion of olefins into platinum-hydrogen bonds. *Inorg. Chem.* **1974**, *13*, 1541–1543.

(42) Cucciolito, M. E.; De Felice, V.; Panunzi, A.; Vitagliano, A. Five-coordinate olefin complexes of platinum(II) containing sigma-bonded carbon ligands. Coordination environment and stability. *Organometallics* **1989**, *8*, 1180–1187.

(43) Albano, V. G.; Braga, D.; De Felice, V.; Panunzi, A.; Vitagliano, A. Five-coordinate olefin complexes of platinum(II) containing sigma-bonded carbon ligands. Synthesis and characterization of [PtClMe(eta-2-C₂H₄)(N–N')] complexes. Molecular structure of an adduct with a chiral metal center and of its parent four-coordinate complex. *Organometallics* **1987**, *6*, 517–525.

(44) Sanchez, A.; Castellari, C.; Panunzi, A.; Vitagliano, A.; De Felice, V. New cationic five-coordinate monoolefin hydrocarbyl complexes of platinum(II). *J. Organomet. Chem.* **1990**, *388*, 243–252.

(45) LaPointe, A. M.; Rix, F. C.; Brookhart, M. Mechanistic Studies of Palladium(II)-Catalyzed Hydrosilation and Dehydrogenative Silation Reactions. *J. Am. Chem. Soc.* **1997**, *119*, 906–917.

(46) Kocen, A. L.; Klimovica, K.; Brookhart, M.; Daugulis, O. Alkene Isomerization by “Sandwich” Diimine-Palladium Catalysts. *Organometallics* **2017**, *36*, 787–790.

(47) Rix, F. C.; Brookhart, M.; White, P. S. Electronic Effects on the β -Alkyl Migratory Insertion Reaction of para-Substituted Styrene Methyl Palladium Complexes. *J. Am. Chem. Soc.* **1996**, *118*, 2436–2448.

(48) Zhang, Y.; Jian, Z. Polar Additive Triggered Branching Switch and Block Polyolefin Topology in Living Ethylene Polymerization. *Macromolecules* **2021**, *54*, 3191–3196.

(49) Dau, H.; Keyes, A.; Basbug Alhan, H. E.; Ordóñez, E.; Tsogtgerel, E.; Gies, A. P.; Auyeung, E.; Zhou, Z.; Maity, A.; Das, A.; Powers, D. C.; Beezer, D. B.; Harth, E. Dual Polymerization Pathway for Polyolefin-Polar Block Copolymer Synthesis via MILRad: Mechanism and Scope. *J. Am. Chem. Soc.* **2020**, *142*, 21469–21483.

(50) Bamford, C. H.; Brumby, S. Free-radical polymerization of methyl methacrylate in the presence of aluminium chloride. *Makromol. Chem.* **1970**, *134*, 159–167.

(51) Williams, V. A.; Ribelli, T. G.; Chmielarz, P.; Park, S.; Matyjaszewski, K. A Silver Bullet: Elemental Silver as an Efficient Reducing Agent for Atom Transfer Radical Polymerization of Acrylates. *J. Am. Chem. Soc.* **2015**, *137*, 1428–1431.